Rheology of Polyethylenes with Novel Branching Topology Synthesized by a Chain-Walking Catalyst

Rashmi Patil and Ralph H. Colby*

Department of Materials Science and Engineering, Pennsylvania State University, University Park, Pennsylvania 16802

Daniel J. Read*

Department of Applied Mathematics, University of Leeds, Leeds LS2 9JT U.K.

Guanghui Chen and Zhibin Guan*

Department of Chemistry, University of California, Irvine, California 92697

Received June 29, 2005; Revised Manuscript Received October 4, 2005

ABSTRACT: Ethylene pressure was used to vary the molecular architecture of amorphous polyethylenes synthesized with a palladium−bisimine catalyst. At low ethylene pressure, densely branched polymers are formed, and their melt rheology indicates no entanglement even though the weight-average molar mass is 370 000. Polymers produced at higher ethylene pressures have only slightly higher molar masses but show entanglement effects in their rheology. NMR suggests similar levels of short-chain branching (92−97 branches per 1000 carbons) in all the samples. A simple model of polymerization, based on the proposed "chain-walking" mechanism for this catalyst, is used to generate structures via computer simulation. While some of the experimental data are consistent with the predicted molecular structures, there are discrepancies in (i) the scaling of radius of gyration with molecular weight and (ii) the variation of terminal relaxation time with ethylene pressure, both of which suggest long-chain branching, which is not predicted by the computer simulation.

Introduction

Traditional methods to produce dendrimers and hyperbranched polymers use condensation polymerization of AB_2 monomers where branching is introduced by the structure of the monomer.[1] Each addition of monomer increases the number of active sites per chain. In most cases, this conventional approach requires synthesis of a specifically designed monomer. Free radical polymerizations of olefin monomers can have long-chain branching if the catalysts used encourage chain transfer,[2] but this results in broad molar mass distributions.

Without sacrificing the narrow molar mass distribution, single-site metallocene catalysts give excellent control of the stereochemistry and molar mass of polyolefins.[3] Hence, metallocene catalysis can provide a useful tool for studying the influence of polymer architecture on rheological behavior. Brookhart and co-workers[4−6] have demonstrated that catalysts involving late transition metals, such as nickel and palladium−α-diimine catalysts, can lead to branched polyolefins via a "chain-walking" mechanism of catalyst motion along the growing polymer chain. By controlling the kinetic competition between chain-walking and insertion, Guan and co-workers demonstrated that polyethylenes with a continuum of properties can be prepared from homopolymerization of ethylene and suggested that this involved a range of branching topologies from linear to hyperbranched to dendritic.[7−9] The possibility of producing polymers with a continuum of topologies without changing the chemical structure provides a unique opportunity for fundamental studies of topological effects on polymer rheological properties. In this paper we utilize the catalyst, illustrated in Figure 1, which has been extensively studied for polymerization of ethylene by Guan and co-workers.[7−9]

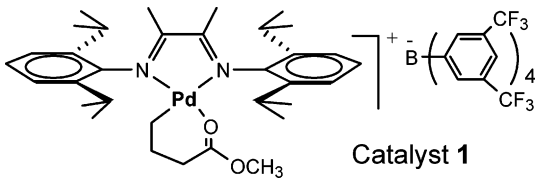

Figure 1. Ethylene coordination polymerization is catalyzed by this Pd−α-diimine complex.

According to the proposed "chain-walking" mechanism,[4−9] the catalyst remains attached to the growing chain for the duration of the polymerization and grows the chain via the following set of basic events: (i) ethylene coordination and dissociation, in which an ethylene molecule is trapped or released by the catalyst, (ii) ethylene insertion, in which the trapped ethylene molecule is added to the chain at the site currently occupied by the catalyst, (iii) isomerization (chain-walking) in which the catalyst can "walk" to an adjacent site on the polymer chain, and (iv) chain transfer, which is thought to be rare. Because the location of the catalyst controls the position of the next monomer addition, nonlinear chain propagation (branching) occurs when monomers add after the catalyst has "walked" to the middle of a chain strand. The chain-walking process can be regulated by ethylene pressure, and thus the topology can be varied from a nearly linear structure with sparse branching to a densely branched structure by simply changing the ethylene pressure P.[7−9]

The plateau modulus, G_N^0, is an important material parameter and is one of the characteristic constants for each type of polymer melt. It reflects the molecular architecture of the polymer and determines the entanglement molar mass M_e. The plateau modulus can also be correlated with unperturbed chain dimen-

10.1021/ma051408p CCC: $30.25
Published on Web 11/12/2005

sions,[1,10] such as the radius of gyration R_g. For linear polyethylene[10] (PE), $G_N^0 = 2.60$ MPa and $M_e = 1040$. For the polymers produced by the catalyst in Figure 1, the plateau modulus is more pronounced at high ethylene pressure because sparser branching allows the polymers to interpenetrate and entangle more. If the connection between molecular architecture and rheology can be understood, the desirable ability to tailor both processing and end-use properties in, for example, polyethylene film becomes a possibility. The objectives of this research were the synthesis and molecular and rheological characterization of PEs with similar high molar masses and narrow molar mass distributions to determine the influence of branching structure on rheological properties.

We first discuss the results of a simple computer simulation of the polymerization (details are in the Appendix) that provide pictures of the architectures produced by our polymerization. We then present the synthesis, molecular characterization, and rheology of the branched polyethylenes we have made. Connections are then made between rheology and molecular structure.

Polymerization Simulation

When considering the experimentally determined properties of the polymers in this study, it is useful to have in mind the possible molecular structures that might be formed at different ethylene pressures, which are consistent with the proposed chain-walking mechanism for the polymerization.[4−9] To this end, we have performed stochastic simulations of the chain growth based upon this simple mechanism. Our simulation is described in the Appendix and requires just two parameters, which are the probability of adding a monomer when the catalyst is at a chain end (thus growing linear chain) or of adding a monomer when the catalyst is in the middle of a chain section (thus adding a branch point). If a monomer is not added, then the catalyst "walks" to an adjacent carbon. As described in the Appendix, the ratio of these probabilities determines the branching density and is held fixed to give a branching density of about 100 branches/1000C. The magnitudes of these probabilities vary with ethylene pressure, and this controlling parameter changes the global structure of the polymers made. Different simulations are performed with different "normalized pressure" $\tilde{P}$ relative to some (unknown) reference pressure, P_{ref}.

These simulations are very similar in structure to those described previously by Chen et al.[11] and by Michalak and Ziegler.[12] These authors include several parameters that allow detailed prediction of the exact proportions of different types of short chain branches, for comparison with NMR data. This paper is concerned predominantly with rheology and light scattering, which are sensitive to the large-scale shape of the polymers. The simple simulation outlined above allows us to focus on the few key parameters that affect the large-scale polymer shape but do not reproduce the NMR data. We did some test simulations with additional parameters as used by Chen et al.[11] and found that there was no qualitative difference in the results reported below—for the purposes of clarity, we have omitted these extra parameters in the subsequent discussion.

To characterize the type of large-scale structures being formed at different molar masses by our algorithm, we began by calculating the radius of gyration

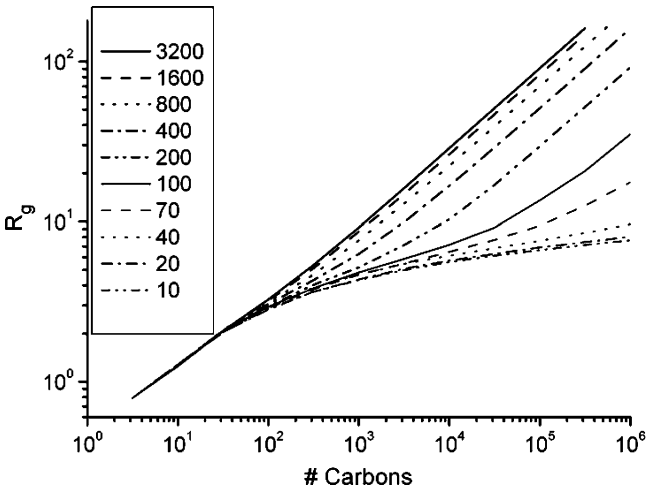

Figure 2. Simulation results for the dependence of radius of gyration on number of carbons, assuming chain-walking for normalized ethylene pressure $\tilde{P}$ varying from 10 to 3200.

of the structures, assuming ideal Gaussian chain conditions (i.e., neglecting the swelling effect due to excluded volume). Although this is not particularly realistic as regards modeling the solution properties of the molecules, it is a quick way of identifying the molecular structure that is formed and avoids lengthy Monte Carlo simulation of the accessible configurations of large molecules.

Figure 2 is a log−log plot of the radius of gyration vs number of carbons for molecules made at a range of values of the pressure parameter, $\tilde{P}$. (These curves represent an average over 50 different molecules made at each pressure.) These curves typically show three distinct regimes. At low molar masses, there is a small region with slope of (roughly) $^1/_2$, indicative of short, predominantly linear chains with essentially no branches. Above 10 carbons (recall, the branching density $\lambda = 0.1$) the curve adopts a shallower slope, indicating a branched structure. However, at higher molar masses the slope increases back to $^1/_2$, indicating that at the largest scales the structure becomes linear again. We find that, in the initial linear and branched regimes, the radius of gyration as a function of molar mass is determined *only* by the branching density. As ethylene pressure is varied, the crossover to the high molar mass region is changed, and at sufficiently high pressure the branched regime is absent altogether. We believe that the high molar mass "linear" regime is present at *all* pressures, provided one looks to sufficiently high molar masses. These observations are consistent with, but add detail to, earlier works[11,12] which indicate that the structure becomes "more linear" and has a larger radius of gyration as ethylene pressure is increased.

Figures 3 and 4 show, at various molar masses, molecules growing at $\tilde{P} = 100$ and $\tilde{P} = 400$, respectively. These illustrate the last two regimes of growth. (The eventual linear structure is emphasized by slightly biasing the step direction of the bonds.) In the second, branched regime, the catalyst is able to diffuse (via chain-walking) over the whole molecule as it adds monomers to the growing structure. The crossover from the second to the third regime occurs when, as the molecule gets larger, the catalyst does not have time to walk over the whole molecule as it adds more monomers and so gets stuck on one side of the molecule. More quantitatively, we believe that the crossover occurs at

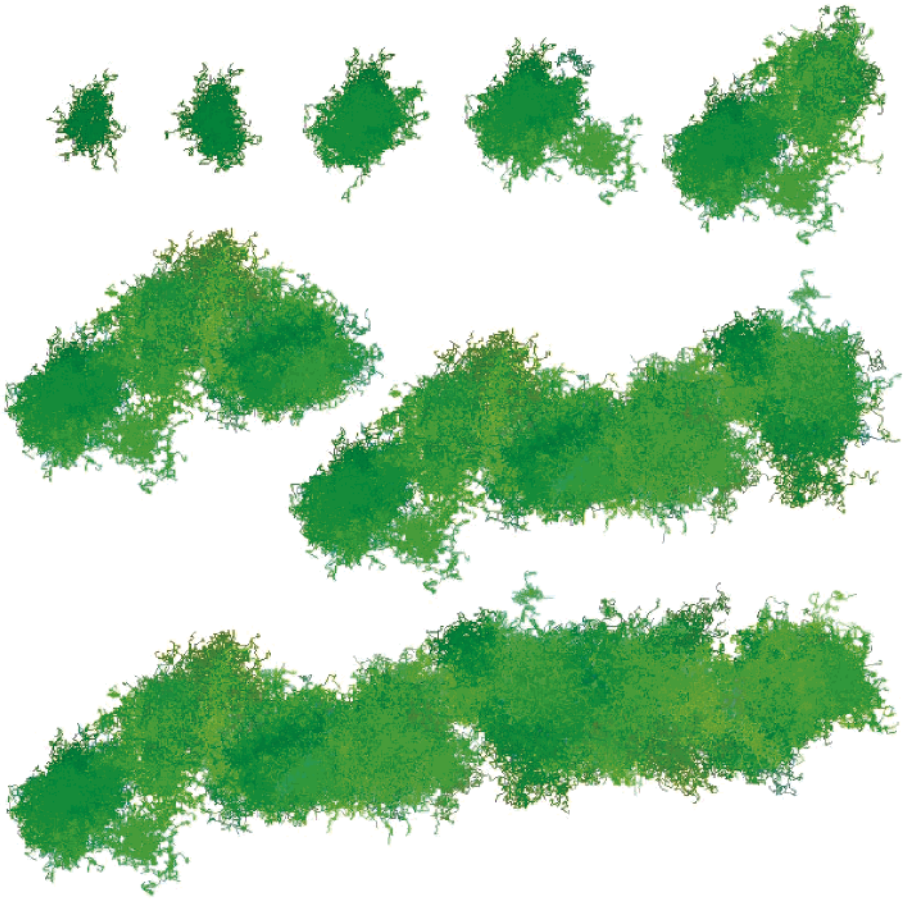

Figure 3. Simulated polymers produced at normalized ethylene pressure $\tilde{P} = 100$ (cf. Figure 2). The polymerization proceeds from the upper left to the lower right, as polymers have 2000, 4000, 10 000, 20 000, 40 000, 100 000, 200 000, and 400 000 carbons.

degree of polymerization N, where the catalyst walking time over a molecule of this size equals the time to add the next N monomers. Increasing ethylene pressure increases the rate of monomer addition and so pushes the crossover to lower molar mass (compare Figures 3 and 4). From then onward, the catalyst is rarely able to retrace its path back along the whole molecule, so monomers are only ever added to one side of the molecule, and ultimately a large-scale linear structure (albeit highly branched at a local level) is formed.

The samples in this study are all made with roughly the same molecular weight (with roughly 26 000 carbons) but at different ethylene pressures. On the basis of these simulations, we would anticipate that at low ethylene pressures the molecules have a highly branched, globular structure. On increasing the pressure, at fixed molecular weight, the structure should become globally "linear", i.e., the locally branched "sausage-like" structure shown in Figure 3. Further pressure increases lead the "sausage" to become longer and thinner, giving an increase in radius of gyration. There is no evidence in the simulations for an intermediate "hyperbranched" structure (i.e., long linear-like sections joined by sparse long-chain branches), as has been suggested previously.[7,8]

Experimental Section

Polymerization Procedure.[4−9] The chain-walking catalyst used in our ethylene polymerization, catalyst 1 (Figure 1), was prepared by following a literature procedure.[5,6] Ethylene polymerization was performed in a Parr pressure reactor equipped with mechanical stirring and temperature control. A typical polymerization procedure is described as follows: The Parr reactor was preheated to 100 °C for 2 h under vacuum and then cooled under N_2 to room temperature before use. A preprepared catalyst 1 solution in chlorobenzene/toluene (1:3) was transferred into the Parr reactor under N_2. After purging the reactor with N_2 and ethylene, the system was filled with ethylene to the desired pressure, and polymerization was allowed to continue at room temperature for 48 h. The polymerization was quenched by addition of excess triethylsilane under N_2. The solution was passed through Celite and neutral alumina gel to remove residual catalyst and then concentrated in vacuo. The polymer was finally precipitated in methanol or acetone and dried under vacuum.

SEC-MALLS Characterization of Copolymers.[7,8] All the polymers were characterized by size-exclusion chromatography (SEC) coupled to a multiangle laser light scattering detector (MALLS) for obtaining both the weight-average molar mass (M_w) and the z-average radius of gyration (R_g). Measurements were made on dilute fractions eluting from a SEC consisting of a HP Aglient 1100 solvent delivery system/auto injector with an online solvent degasser, temperature-controlled column compartment, and an Aglient 1100 differential refractometer. A Dawn DSP 18-angle light scattering detector (Wyatt Technology, Santa Barbara, CA) was coupled to the SEC to measure both M_w and R_g for each fraction of the polymer eluted from the SEC column. A 30 cm column was used (Polymer Laboratories PLgel Mixed C, 5 μm particle size) to separate polymer samples. The mobile phase was uninihibited tetrahydrofuran, for which polyethylenes have $dn/dc = 0.078$ mL/g and the flow rate was 0.5 mL/min. Both the column and the differential refractometer were held at 35 °C. 60 μL of a 2 mg/mL solution was injected into the column. Acetone (0.2%) was used as an internal flow marker. Results for M_n, M_w, M_z, M_w/M_n, and R_g are listed in Table 1.

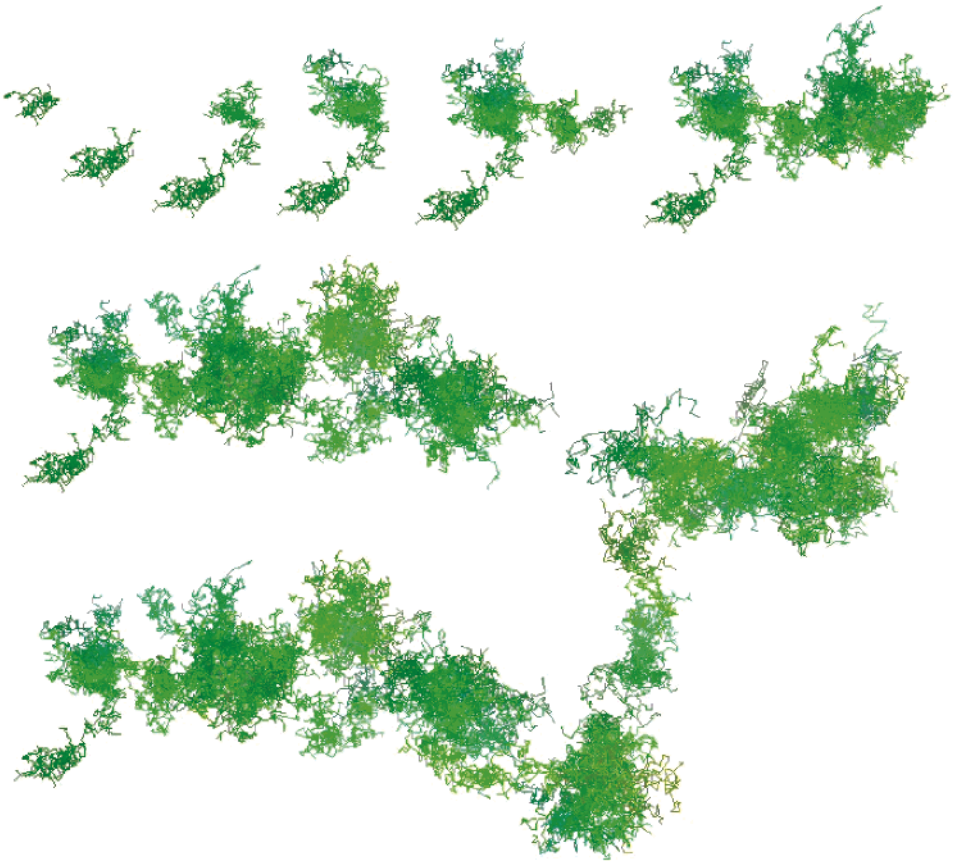

Figure 4. Simulated polymers produced at normalized ethylene pressure $\tilde{P} = 400$ (cf. Figure 2). The polymerization proceeds from the upper left to the lower right, as polymers have 200, 400, 1000, 2000, 4000, 10 000, 20 000, and 40 000 carbons.

Table 1. Characterization Results

pressure (atm)	0.1	0.3	1.0	10.2	34.0
M_n	235K	330K	318K	378K	447K
M_w	373K	441K	481K	486K	518K
M_z	553K	603K	705K	643K	592K
M_w/M_n	1.58	1.33	1.51	1.28	1.16
R_g (nm)	13.0	16.4	23.5	25.9	31.2
branches/1000 CH_2	97	97	96	95	92
T_g (°C)	−75	−68	−67	−65	−56
η_0 (Pa s) at 30 °C	114	125	67000	5.7×10^6	1.1×10^8
G_N^0 (MPa) at 0 °C				0.10	0.74

DSC Determination of Glass Transition. Glass transition temperature (T_g) of the PE samples was determined using a Perkin-Elmer differential scanning calorimeter (Pyris 6). The PE samples were prepared for DSC measurements by drying under vacuum at 60 °C for 3 days. Liquid nitrogen was used as coolant, and nitrogen was used as purging gas for the experiments. The scanning temperature range was −90 to 200 °C at a scanning rate of 10 °C/min. Results for T_g are listed in Table 1.

NMR Determination of Branching Density. NMR spectra were recorded on Bruker DRX400, Bruker GN500, or Bruker Omega500 MHz FT-NMR instruments. The PE samples were prepared for NMR measurements by drying under vacuum at 60 °C for 3 days and then dissolved in deuterated chloroform ($CDCl_3$) at a concentration of 10 mg/mL.

Branching density of the PE samples was determined from their NMR spectra using literature methods.[13] Since one branching point on the polymer chain will inevitably result in one more end methyl group $-CH_3$ (no loop structure), the branching density per 1000 carbons can be determined by measuring the number of methyl groups per 1000 carbons from ^{1}H NMR spectra. Protons from CH_3 groups can be precisely determined because they are clearly separated from protons from CH and CH_2 groups. The branching density N_{br} (branches per 1000 carbon atoms) is reported in Table 1, calculated based on the following equation:

$$N_{br} = \frac{500\left[\frac{\text{no. of } CH_3 \text{ protons}}{3} - 2\right]}{\text{total no. of protons}} \quad (1)$$

Rheology. The PE samples were prepared for rheology measurements by drying under vacuum at 60 °C for several days, followed by compression-molding an 8 mm diameter, ~1 mm thick disk at 80 °C, for solidlike samples synthesized at high P. Samples synthesized at low P were sufficiently fluid at room temperature to be poured directly onto the bottom plate of the rheometer after drying. Oscillatory shear tests were performed using a Rheometrics strain-controlled ARES rheometer. The angular frequency ω was varied from 10^2 to 10^{-4} rad s^{-1}, and the temperature ranged from −60 to 70 °C. The temperature was decreased in 30 K increments at high temperatures and at 5 K intervals at temperatures approaching T_g. All PE samples were studied under a nitrogen atmosphere in order to minimize thermooxidative degradation. The isothermal rheology data at different temperatures were shifted to obtain master curves at the reference temperature $T_0 = 30$ °C using time−temperature superposition.[1]

Results

Linear and branched structures have different swollen fractal dimensions[1] and consequently exhibit different exponents on plots of log R_g vs log M_w. Linear polymers have exponent $\nu \equiv \mathrm{d}(\log R_g)/\mathrm{d}(\log M_w) \approx 3/5$, while branched polymers have exponent $\nu \approx 1/2$ in good solvent. While NMR shows that the branching density is similar in all samples, the increase in R_g with ethylene pressure indicates a change in the arrangement of these branches, toward a more open structure with increasing ethylene pressure. This is seen in Figure

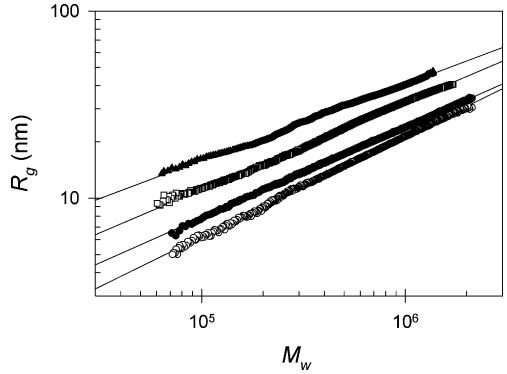

Figure 5. Correlation of radius of gyration with weight-average molar mass (both obtained from SEC-MALLS) for polyethylene samples made at 0.1 atm (open circles; $\nu = 0.53$), 0.3 atm (filled circles, $\nu = 0.48$), 1.0 atm (open squares; $\nu = 0.46$), and 34 atm (filled triangles; $\nu = 0.41$, all exponents with uncertainties of ± 0.02).

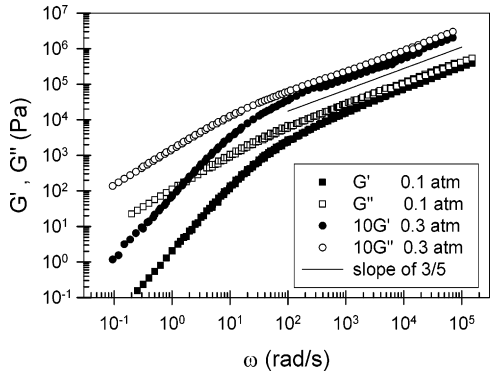

Figure 6. Master curves of the frequency dependence of storage modulus $G'(\omega)$ (filled symbols) and loss modulus $G''(\omega)$ (open symbols) of unentangled samples synthesized at ethylene pressures of 0.1 atm (squares) and 0.3 atm (circles) at the reference temperature $T_0 = 30$ °C. The data for the sample prepared at 0.3 atm have been shifted vertically by a factor of 10 for clarity. The line has the slope 3/5 expected by the Rouse model for a polymer with fractal dimension $D = 3$.

5, where the magnitude of R_g increases with ethylene pressure. We note that the exponent ν *decreases* with ethylene pressure (see the Figure 5 caption for the exponent values). The exponent ν ranges from 0.41 to 0.53, similar to experimental values for randomly branched polymers in good solvent.

Figure 6 shows the frequency dependence of storage and loss moduli, $G'(\omega)$ and $G''(\omega)$, at a reference temperature of 30 °C, for samples made at low ethylene pressure ($P = 0.1$ and 0.3 atm). Densely branched polymers are formed at these low pressures, and the melt rheology indicates no entanglement even though $M_w = 3.7 \times 10^5$. This suggests that the polymers made at low ethylene pressure do not overlap enough to entangle, as there is no hint of any rubbery plateau in Figure 6. The branched polymer Rouse model[1,14] predicts a power law in $G'(\omega)$ and $G''(\omega)$ with exponent determined by the fractal dimension of the polymers (see eq 8.148 of ref 1).

$$G' \sim G'' \sim \omega^{3/(D+2)} \sim \omega^{3/5} \qquad (2)$$

The final result was obtained using the expected fractal dimension of 3, owing to the crowded nature of these highly branched molecules.[15] The line in Figure 6 has slope 3/5, demonstrating that the branched polymer Rouse model describes the linear viscoelasticity of these

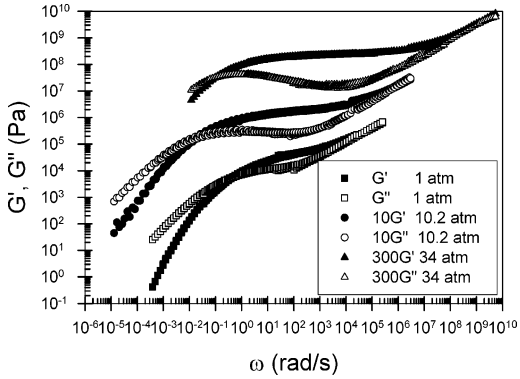

Figure 7. Master curves of the frequency dependence of storage modulus $G'(\omega)$ (filled symbols) and loss modulus $G''(\omega)$ (open symbols) of entangled samples synthesized at ethylene pressures of 1 atm (squares), 10.2 atm (circles), and 34 atm (triangles) at the reference temperature $T_0 = 30$ °C. For clarity, the data for the sample prepared at 10.2 atm have been shifted vertically by a factor of 10, and the data for the sample prepared at 34 atm have been shifted vertically by a factor of 300.

unentangled highly branched polymers. The sample prepared at 0.1 atm has $G' \sim G'' \sim \omega^{0.62\pm0.02}$ for the highest 2 decades of frequency, and the sample prepared at 0.3 atm has $G' \sim G'' \sim \omega^{0.59\pm0.02}$ for the highest 2.5 decades in frequency in Figure 6.

Randomly branched condensation polymers that are not entangled exhibit a power law viscoelastic response[14] qualitatively similar to that observed in Figure 6 at high frequencies (10^3 rad/s $< \omega < 10^5$ rad/s). The frequency exponent of this power law for randomly branched polymers is also understood using eq 2, but with smaller fractal dimension of 2.53, giving a larger frequency exponent of 0.66. Randomly branched polymers also have a much broader (power law) molar mass distribution,[1,14,16] but since the unentangled randomly branched polymers have their dynamics described by the Rouse model[1,14] (with no interactions between chains), the frequency exponent is insensitive to the distribution and only depends on the fractal character of the molecules. Consequently, this simple analysis also holds for our highly branched polymers produced at low pressures, with quite narrow molar mass distributions. The samples made at low ethylene pressure are more like dendrimers, which are also known to not interpenetrate[1] and not entangle.[17,18]

In the melts of densely branched polymers, entanglements do not occur because of the limited possibility of interpenetration between neighboring molecules. The relatively high branching density leads to a compact structure of deformable individual macromolecules. Linear viscoelastic response of randomly branched condensation polymers, with average chain lengths between branch points shorter than $2M_e$, are known to be described by the branched polymer Rouse model.[14] Systems with longer linear chain sections between branch points systematically deviate from the Rouse predictions,[16] presumably indicating the importance of interchain entanglements.

Polymers produced at higher ethylene pressures have only slightly higher molar masses but show entanglement effects in their rheology, presumably because they have a more open structure that allows for interpenetration and interchain entanglement. Figure 7 shows a clear rubbery plateau region in $G'(\omega)$ (in the frequency range 1 rad/s $< \omega < 10^6$ rad/s for the sample made at P

= 34 atm) with weak frequency dependence of $G'(\omega)$ and $G'(\omega) \gg G''(\omega)$, indicating that the polymers produced at high ethylene pressure are entangled. Two easily distinguishable relaxation processes are evident in Figure 7: (1) the transition zone[1] involving segmental relaxation at high frequencies, which separates the glassy modulus of the polymer from the rubbery plateau, and (2) chain relaxation at lower frequencies. Some variations in the transition zone are caused by the observed differences in glass transition temperatures (see Table 1).

The appearance of a rubbery plateau in Figure 7 indicates an elastic character of the polymer melt, caused by chain entanglement. However, the plateau modulus seen is much lower than that of linear PE. For example, Figure 7 shows that the sample made at an ethylene pressure $P = 34$ atm is strongly entangled, with a plateau modulus of order 1 MPa, somewhat lower than conventional polyethylene ($G_N^0 = 2.6$ MPa) because of the high level of short chain branching (roughly every 10th carbon atom). The molar mass of an entanglement strand,[1] M_e, can be calculated from the plateau modulus

$$M_e = \frac{\rho RT}{G_N^0} \tag{3}$$

where R is the universal gas constant ($R = 8.314$ J mol^{-1} K^{-1}), ρ is the density of the polymer at temperature T, and G_N^0 is the plateau modulus. Since the plateau modulus is lower, the values of M_e obtained are larger than conventional linear PE. Only the samples made at the highest ethylene pressures had rubbery plateaus that were sufficiently well-defined to exhibit a minimum in G'', and the plateau modulus was estimated as the value of G' at the frequency where G'' shows a local minimum (see Table 1). For the sample made at an ethylene pressure of 34 atm, $G_N^0 = 0.74$ MPa at 0 °C and $M_e = 2500$, while the sample made at an ethylene pressure of 10.2 atm has $G_N^0 = 0.10$ MPa at 0 °C and $M_e = 18\,000$.

Time−temperature superposition works very nicely for the samples prepared at low ethylene pressures (Figure 6) but works more poorly as ethylene pressure is increased (Figure 7). Failure of superposition was observed most clearly for $G''(\omega)$ in the plateau region of the samples made at high ethylene pressures. Since NMR suggests similar levels of short-chain branching (92−97 branches per 1000 carbons) in all the samples, large-scale architectural differences in structure must account for differences in entanglement and time−temperature superposition in these branched polyethylenes. As ethylene pressure is increased, subtle changes in chain overlap with temperature apparently affect the extent of entanglement slightly.

The frequency dependence of $|\eta^*(\omega)|$ (magnitude of complex viscosity) is plotted in Figure 8 for four representative samples at a reference temperature of 30 °C. The low shear rate value of the complex viscosity is the zero-shear-rate viscosity η_0. Table 1 lists the values of η_0 at 30 °C for the various samples studied: The zero-shear-rate viscosity increases by 6 orders of magnitude when the ethylene pressure is increased, even though the molar mass is nearly constant, as shown in Figure 9. We can understand the increase in viscosity for the entangled polymers with a simple scaling argument. The simulations suggest that the overall architecture

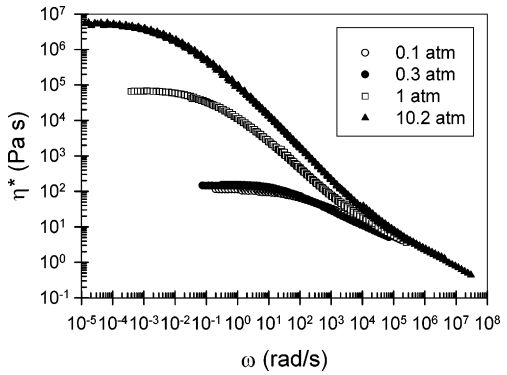

Figure 8. Frequency dependence of the complex viscosity at 30 °C, for samples synthesized at ethylene pressures of P = 0.1, 0.3, 1.0, and 10.2 atm.

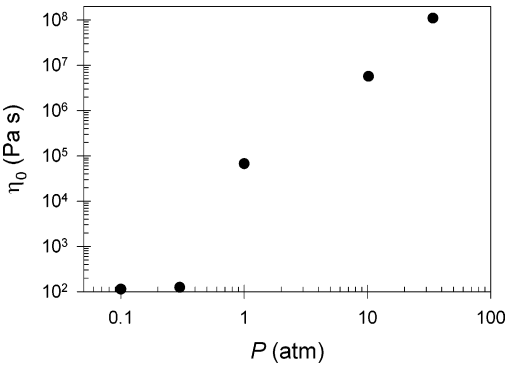

Figure 9. Dependence of zero-shear-rate viscosity at 30 °C on the ethylene pressure used in synthesis.

of these polymers is a linear backbone with considerable amounts of short-chain branched fuzz. Since the branching is roughly every 10 carbons, and polyethylene has 75 carbons per entanglement strand, the branching is too dense to allow entanglements to form in the fuzz. We therefore envision only the linear backbones being able to entangle, and the fuzz simply acts to dilute the backbones, giving the backbones an effective volume fraction ϕ. This volume fraction can be directly determined from the experimental plateau modulus G_N^0

$$\phi^2 = \frac{G_N^0}{G_0} = \frac{M_{e,0}}{M_e} \tag{4}$$

where $G_0 = 2.60$ MPa is the plateau modulus of linear polyethylene,[10] M_e is the experimental value of the entanglement molar mass, and $M_{e,0} = 1040$ is the molar mass of an entanglement strand for linear polyethylene.[10] On the basis of the measured plateau moduli and eq 4, we conclude that $\phi = 0.64$ for the sample prepared at 34 atm and $\phi = 0.24$ for the sample prepared at 10.2 atm. This backbone volume fraction also affects the end-to-end distance of the backbone R and assuming Gaussian statistics, $R^2 \sim \phi M$. The radius of gyration data in Figure 5 suggest the sample prepared at 34 atm has roughly twice the size of the sample prepared at 1 atm, suggesting a crude estimate for the backbone volume fraction of the 1 atm sample, $\phi \approx 0.64/2^2 = 0.16$. This estimate is consistent with the expectation of eq 4, based on an apparent plateau modulus of $G_N^0 = 70\,000$ Pa for the 1 atm sample in Figure 7. The tube diameter a is determined from random walk statistics along the backbone, with effective entanglement molecular weight along the backbone $M_{e,bb}$ smaller than M_e by a factor

that is the backbone volume fraction ϕ.

$$a^2 \sim M_{e,bb} = \phi M_e = \frac{M_{e,0}}{\phi} \tag{5}$$

Reptation of the linear backbones (covered with fuzz) occurs by curvilinear diffusion along the tube of contour length $L = Ma/M_e$ with curvilinear diffusion coefficient D_c that depends on M but not ϕ. The tube disengagement time[1]

$$\tau = \frac{L^2}{D_c} \sim \frac{M^2 a^2}{M_e{}^2 D_c} \sim \phi^3 \tag{6}$$

is the longest relaxation time in the polymer melt. The product of the relaxation time and the plateau modulus determines the melt viscosity

$$\eta = G_N^0 \tau \sim \phi^5 \tag{7}$$

which scales as the fifth power of the volume fraction. This explains the factor of 1000 change in the viscosity of the entangled samples in Figure 9 when the ethylene pressure is changed from 1 to 34 atm, as $(0.64/0.16)^5 = 1000$.

Comparison of Simulations and Experiments. At a qualitative level, there are a number of aspects of the experimental results that seem very consistent with the predicted molecular structures emerging from the simulations. Simulations suggest that the branching density should remain constant with ethylene pressure, which is observed. The predicted "globular" structures at low ethylene pressure would be anticipated to exhibit unentangled polymer rheology, as is the case. At higher pressures, the simulations predict a linear structure, which is highly branched at a local level but which gets longer and thinner with increasing pressure. One would expect, as the molecules become globally more "linear", that they would begin to become entangled in the melt state and that the longer, thinner structures would have a higher plateau modulus. This is very consistent with the increasing plateau modulus and decreasing entanglement molecular weight observed with increasing pressure in the experiments. Finally, the simulations indicate an increasing radius of gyration with increasing ethylene pressure, and this is observed in light scattering results.

Nevertheless, several puzzles remain in the experimental data that we have not been able to account for. The light scattering results are taken in good solvent conditions. The observed slope in the plot (Figure 5) of log R_g vs log M_w is about 0.5 at the lowest pressure, *decreasing* to about 0.41 at the highest pressure. In good solvent conditions, a slope of 0.5 is indicative of a branched, not a linear, structure. In the simulations, the slope is always predicted to *increase* with increasing pressure, toward a value commensurate with a linear topology (such a slope would be about 3/5 in good solvent). Thus, there is no experimental evidence of large-scale linear structures in the light scattering data.

There are also unexplained features in the rheological measurements. The polymer made at 10.2 atm has a plateau modulus roughly a factor of 7 lower than the 34 atm polymer. Despite this, its terminal time appears to be roughly a factor of 10 larger than the 34 atm polymer. This observation is very difficult to explain using conventional tube models for entangled linear polymers; one would expect that the polymer with the lower entanglement molecular weight would lie within a longer, thinner tube and consequently have a longer terminal time. It might be that there are some "long chain branches" in the 10.2 atm polymer, which would explain the larger terminal time. Some qualitative evidence for this is also present in the broad width of the "peak" in the loss modulus. However, long chain branches are not really consistent with the polymerization simulations based on the chain-walking mechanism.

A final puzzle lies in the rate at which the polymer properties change with increasing ethylene pressure. According to the simulations (see Figure 2), for polymers with between 10^4 and 10^5 carbons, most of the structural changes occur between $\tilde{P} = 40$ and $\tilde{P} = 1600$, a factor of (roughly) 40 in pressure. Outside this range, the simulations predict very small changes occur in the global structure for the molar masses studied in the experiments. In the experiments, however, the structure appears to vary continuously between polymers made at pressures of 0.1 atm and those made at 34 atm, a factor of 340 in pressure. This discrepancy might be explained by non-first-order reaction kinetics with respect to ethylene pressure. Taken together, there are enough discrepancies to prevent the molecular structures emerging from the stochastic simulation being used to predict the polymer properties. This leads us to question whether there is important science missing from the simulations in their present form.

One important ingredient that is lacking is the effect of excluded volume. This will affect the radius of gyration in the solution state. (Chen et al.[11] addressed this issue for relatively smaller molecules with, typically, 5000 carbons.) Excluded volume could also affect the polymerization process itself. In highly branched structures, excluded volume might prevent the bulky catalyst from walking to all possible sites. By inhibiting chain-walking, excluded volume would slow down catalyst diffusion along the polymer contour. This creates more linear structures, since the catalyst does not diffuse as far before the next reaction. These suggestions are borne out by some simple test simulations we have performed, in which polymers are laid down on a cubic lattice and the catalyst is prevented or discouraged from walking to "crowded" sites on the lattice. However, a fully realistic simulation, in which both the catalyst and growing polymer are given sensible dynamics, would be quite costly and is beyond the present investigation.

However, including excluded-volume effects does not even qualitatively account for two of the above discrepancies: the slope of log R_g vs log M_w (which indicates a globally branched, rather than a linear, structure) and the relatively large terminal time of the 10.2 atm polymer (which is also suggestive of some large-scale branching). The chain-walking mechanism alone cannot predict structures that are branched on a large scale; it leads only to linear structures, as shown in Figures 2, 3, and 4. The experimental evidence we have at present is therefore suggestive of the need for some mechanism in addition to chain-walking during the polymerization process.

Conclusion

The molecular structure and rheology of branched polyethylenes synthesized with a palladium-bisimine catalyst change systematically with ethylene pressure.

Low ethylene pressures allow the catalyst to walk extensively along the molecule between additions of ethylene and produce densely branched polymers that do not entangle. The linear viscoelastic response of these unentangled densely branched polymers is well described by the Rouse model. As ethylene pressure is increased, ethylene addition occurs faster, not allowing the catalyst time to walk as far, leading to more open structures that form entanglements in the melt. Our current understanding of the chain-walking mechanism suggests that the molecules produced at high ethylene pressures should be densely branched on their smallest scales, and be linear on their largest scales, with no long-chain branching. However, both the swollen fractal dimension of the molecules and their rheology suggest that long-chain branching effects are observed. Consequently, mechanisms other than chain-walking should be considered in the polymerization.

Acknowledgment. This material is based upon work supported by the U.S. Army Research Laboratory and U.S. Army Research Office under Grant DAAD19-02-1-0275 Macromolecular Architecture for Performance (MAP) MURI. Z.G. thanks the National Science Foundation (DMR-0135233) for financial support of this work.

Appendix: Computer Simulation

A molecule is grown as follows: when the catalyst is attached to a given carbon, I, there is a site-dependent probability p_I that the next significant action of the catalyst is to add a monomer to that site. The alternative, with probability $1 - p_I$, is to "walk" to an adjacent carbon in the same molecule, chosen randomly from its neighbors. We distinguish between three different sites on the molecule. If the catalyst is at a chain end (i.e., a carbon with one neighbor), then the addition of a monomer (with probability p_{end}) continues the growth of a linear section of chain. If the catalyst is in the middle of a linear section of chain (i.e., a carbon with two neighbors), then the addition of a monomer (with probability p_{mid}) adds a side branch. If the catalyst is on a branch point (i.e., a carbon with three neighbors), then we do not allow monomer addition—the catalyst jumps to one of its neighbors. This algorithm allows the growth of a molecule up to a specified number of carbons and requires just two parameters, p_{end} and p_{mid}.

The probabilities p_{end} and p_{mid} vary with ethylene pressure; we can predict the form of this variation using a simple kinetic model. The catalyst is thought to exist in two states: a trapped state (T) in which it traps an ethylene monomer, with the possibility of adding it to the growing chain, and an untrapped state (U) in which it might walk to an adjacent site.[7–9] Beginning in the untrapped state U, a catalyst might walk to an adjacent site U′ or trap a monomer. These can be represented schematically as

$$\mathrm{U} \rightarrow \mathrm{U}' \qquad k_{\mathrm{W},I}$$
$$\mathrm{U} \rightarrow \mathrm{T} \qquad k_{\mathrm{T},I}P$$

where $k_{\mathrm{W},I}$ and $k_{\mathrm{T},I}$ are the rate constants for the two processes for site I, and the rate of the second process is proportional to ethylene pressure P. Hence, in the U state, the probabilities of "walking" or "trapping" are

$$p_{\mathrm{W},I} = \frac{k_{\mathrm{W},I}}{k_{\mathrm{W},I} + k_{\mathrm{T},I}P}$$
$$p_{\mathrm{T},I} = \frac{k_{\mathrm{T},I}P}{k_{\mathrm{W},I} + k_{\mathrm{T},I}P}$$

In the trapped state, T, the monomer might be added to the chain or dissociate from the catalyst, represented as

$$\mathrm{T} \rightarrow \sim\mathrm{U}'' \qquad k_{\mathrm{A},I}$$
$$\mathrm{T} \rightarrow \mathrm{U} \qquad k_{\mathrm{D},I}$$

where the notation $\sim$U″ is used to indicate a new unbound state in which a monomer has just been added. In the T state, the probabilities of "addition" or "dissociation" are

$$p_{\mathrm{A},I} = \frac{k_{\mathrm{A},I}}{k_{\mathrm{A},I} + k_{\mathrm{D},I}}$$
$$p_{\mathrm{D},I} = \frac{k_{\mathrm{D},I}}{k_{\mathrm{A},I} + k_{\mathrm{D},I}}$$

Starting from a given U state, there are hence three possibilities, all of which return the catalyst to a U state: walking, trapping followed by monomer addition, and trapping followed by dissociation. The latter returns the catalyst to the original U state and so does not constitute a significant "action". Hence, the probability p_I of monomer addition being the next significant action, starting from the U state, is

$$p_I = \frac{p_{\mathrm{T},I}p_{\mathrm{A},I}}{1 - p_{\mathrm{T},I}p_{\mathrm{D},I}} = \frac{r_I\tilde{P}}{1 + r_I\tilde{P}} \tag{8}$$

where

$$r_I = \frac{p_{\mathrm{A},I}k_{\mathrm{T},I}P_{\mathrm{ref}}}{k_{\mathrm{W},I}}$$

and

$$\tilde{P} = \frac{P}{P_{\mathrm{ref}}}$$

Here, P_{ref} is a reference pressure. Hence, if we specify r_{end} and r_{mid} at some low value of the reference pressure, then eq 1 indicates how p_{end} and p_{mid} will vary with normalized pressure, $\tilde{P}$.

It is clear, from the above equations, that increasing ethylene pressure increases the rate of monomer addition relative to the rate of chain-walking. At sufficiently low pressures chain-walking will be the dominant mechanism, so that the catalyst will sample many "mid" and "end" sites during the addition of monomers. In this limit, we obtain a simple formula relating the branching density, λ (defined here as the number of branches per carbon), to the simulation parameters p_{end} and p_{mid}. In a highly branched structure, a fraction λ of carbons are branch points, another fraction λ of carbons are "end"

sites, and the remaining fraction $(1 - 2\lambda)$ are "mid" sites. Assuming the catalyst samples an average over these sites when adding monomers, the rate of increase of number B of branch points and N of carbons with simulation steps n is

$$\frac{dB}{dn} = p_{mid}(1 - 2\lambda)$$

$$\frac{dN}{dn} = 2[p_{mid}(1 - 2\lambda) + p_{end}\lambda]$$

At steady state, we must have $\lambda = dB/dN$, which gives a quadratic formula for λ that we solve to obtain

$$\lambda = \frac{1}{\sqrt{\frac{p_{end}}{p_{mid}}} + 2} \tag{9}$$

In the simulations reported in this paper, we set $r_{end} = 0.000\,62$ and $r_{mid} = 0.000\,01$ and allow $\tilde{P}$ to vary. This gives branching densities of order 0.1 (100 branches per 1000 carbons) in all the simulations reported herein, thereby matching the experiments.

Equation 9 potentially breaks down at the higher pressures when first p_{end} and then p_{mid} approach 1, and monomer addition dominates over chain-walking. One detail that is important here is whether, after the addition of a monomer, the catalyst is attached to the end site on that monomer or to the penultimate carbon. If the catalyst is attached to the end carbon, then eq 9 breaks down when p_{end} approaches 1. If, on the other hand, the catalyst is attached to the penultimate carbon, then eq 9 breaks down at a higher pressure, when p_{mid} approaches 1. In our simulations, we attached the catalyst to the penultimate carbon, so as to preserve a constant value of λ over as large a range of pressure as possible.

References and Notes

(1) Rubinstein, M.; Colby, R. H. *Polymer Physics*; Oxford University Press: New York, 2003.
(2) Billmeyer, F. W. *Textbook of Polymer Science*; Third Edition, Wiley: New York, 1984.
(3) Kaminsky, W.; Arndt, M. *Adv. Polym. Sci.* **1997**, *127*, 143.
(4) Johnson, L. K.; Killian, C. M.; Brookhart, M. *J. Am. Chem. Soc.* **1995**, *117*, 6414.
(5) Johnson, L. K.; Mecking, S.; Brookhart, M. *J. Am. Chem. Soc.* **1996**, *118*, 267.
(6) Mecking, S.; Johnson, L. K.; Wang, L.; Brookhart, M. *J. Am. Chem. Soc.* **1998**, *120*, 888.
(7) Guan, Z.; Cotts, P. M.; McCord, E. F.; McLain, S. J. *Science* **1999**, *283*, 2059.
(8) Cotts, P. M.; Guan, Z.; McCord, E.; McLain, S. *Macromolecules* **2000**, *33*, 6945.
(9) Guan, Z. *J. Polym. Sci., Polym. Chem.* **2003**, *41*, 3680.
(10) Fetters, L. J.; Lohse, D. J.; Colby, R. H. In *Physical Properties of Polymers Handbook,* Mark, J. E., Ed.; AIP Press: New York, 1996.
(11) Chen, Z.; Gospodinov, I.; Escobedo, F. A. *Macromol. Theory Simul.* **2002**, *11*, 136.
(12) Michalak, A.; Ziegler, T. *Macromolecules* **2003**, *36*, 928.
(13) Chen, G.; Ma, X. S.; Guan, Z. *J. Am. Chem. Soc.* **2003**, *125*, 6697.
(14) Lusignan, C. P.; Mourey, T. H.; Wilson, J. C.; Colby, R. H. *Phys. Rev. E* **1995**, *52*, 6271.
(15) Buzza, D. M. A. *Eur. Phys. J. E* **2004**, *13*, 79.
(16) Lusignan, C. P.; Mourey, T. H.; Wilson, J. C.; Colby, R. H. *Phys. Rev. E* **1999**, *60*, 5657.
(17) Uppuluri, S.; Keinath, S. E.; Tomalia, D. A.; Dvornic, P. R. *Macromolecules* **1998**, *31*, 4498.
(18) Uppuluri, S.; Morrison, F. A.; Dvornic, P. R. *Macromolecules* **2000**, *33*, 2551.

MA051408P